PAPER

Measurements of fast-ion losses induced by MHD instabilities using a scintillator-based probe in the HL-2A tokamak

To cite this article: Y.P. Zhang *et al* 2015 *Nucl. Fusion* **55** 113024

IOP Publishing | International Atomic Energy Agency Nuclear Fusion

Nucl. Fusion **55** (2015) 113024 (9pp) doi:10.1088/0029-5515/55/11/113024

Measurements of fast-ion losses induced by MHD instabilities using a scintillator-based probe in the HL-2A tokamak[a]

Y.P. Zhang[1], Yi Liu[1], W. Chen[1], Y. Xu[1], M. Isobe[2,3], D. Li[1], X.Q. Ji[1], Y.B. Dong[1], X.T. Ding[1], G.L. Yuan[1], J.W. Yang[1], X.Y. Song[1], X. Li[1], X.M. Song[1], L.W. Yan[1], Q.W. Yang[1], X.R. Duan[1] and the HL-2A Team

[1] Southwestern Institute of Physics, PO Box 432, Chengdu 610041, People's Republic of China
[2] National Institute for Fusion Science, 322-6 Oroshi-cho, Toki 509-5259, Japan
[3] The Graduate University for Advanced Studies (SOKENDAI), 322-6 Oroshi-cho, Toki 509-5292, Japan

E-mail: zhangyp@swip.ac.cn

Received 18 March 2015, revised 31 August 2015
Accepted for publication 4 September 2015
Published 5 October 2015

Abstract

Characteristics of fast-ion losses induced by various magnetohydrodynamic (MHD) instabilities, such as tearing mode (TM), long-lived mode (LLM), and sawtooth crash, have been observed and experimentally investigated in the HL-2A tokamak. To study fast-ion losses, a new scintillator-based lost-fast ion probe has been developed and used, and an increment of the fast-ion loss rate as the MHD amplitude increase has been measured. Compared with TM and LLM, the fast-ion losses induced by sawtooth crash have a broad range in energy and pitch angle. There may be some interactions between fast ions and magnetic disturbance, which cause the losses with a wide range of energy and pitch angle. During disruptions, the total neutron emission rate drops by ~90% as a result of the strong fast-ion losses. The possible reasons for this phenomenon are the strong magnetic perturbations and the drastic change of the fast-ion transport. In addition, the clear experimental evidence of drastic losses of fast ions during disruptions have been obtained.

Keywords: fast ion, fast-ion loss probe, MHD, NBI, tokamaks

(Some figures may appear in colour only in the online journal)

1. Introduction

Since the good confinement property of fast ions is an essential requirement for the realization of an ignited fusion reactor, the behaviour of fast ions in magnetically confined fusion plasmas is one of the important research subjects in fusion studies [1–3]. Self-maintained D–T burning plasma can be realized under the condition that fusion-born energetic α-particles are confined long enough to heat the bulk plasma [4]. In order to perform effective bulk plasma heating, losses of α-particles should be suppressed down to an acceptable level. If α-particles are substantially lost from the plasma due to various reasons, the self-maintained state will be inevitably terminated [5]. At present, fast ions are mainly generated by plasma auxiliary heating systems such as neutral beam injection (NBI) and ion cyclotron resonance heating (ICRH), which will support the plasma operation by additional heating. For efficient plasma heating, good confinement of the fast ions is required. Significant losses of fast ions will reduce the heating efficiency and NBI current drive [6]. Furthermore, the localized heat load on the plasma facing components (PFCs) due to the impact of the significant escaping fast ions may damage drastically the PFCs or pollute the plasma in large fusion devices like the International Tokamak Experimental Reactor (ITER) [7]. Understanding the behaviour of fast ions is therefore crucial. In particular, a good confinement of the fast ions is essential to achieve a high fusion power gain, an essential element of the ITER project.

[a] Contributed paper, *25th IAEA Fusion Energy Conf. (Saint Petersburg, Russia, 13–18 October 2014)* EX/P7-24.

Fast-ion losses due to MHD instabilities have been extensively studied theoretically [8] and experimentally [5, 9] in magnetic fusion devices. There are two primary fast-ion loss mechanisms related to the magnetic disturbance. The first arises from the use of a finite number of toroidal field (TF) coils to generate the toroidal magnetic field. This leads to a so-called TF ripple, causing banana drift and/or TF ripple trapping. In the rippled field, the orbits of toroidally trapped banana ions are not closed and their turning points experience a small, but finite vertical displacement after each bounce. When the ripple amplitude is large, fast ions are lost within a few hundred bounces, a time much shorter than their slowing down time. If the TF ripple well is deep enough, the TF ripple trapping can occur, leading to rapid losses of fast ions. The other type of magnetic disturbance that can result in fast-ion losses is self-generated and arises from MHD instabilities. Additional heating and fusion reactions produce large amounts of fast ions in the plasma core. MHD instabilities can often be driven by these ions, which in turn can often cause the redistribution of the energetic particles and even anomalous losses. In addition, MHD instabilities driven by the bulk plasma can potentially induce the redistribution and losses of fast ions. Numerous efforts have been dedicated to studying the fast-ion transport and the interplay of fast ions and MHD modes [10–13]. It has been experimentally observed that significant redistribution and/or losses of energetic ions are caused by sawteeth [14]. A reduction in NBI current drive efficiency caused by beam-ion losses due to tearing mode (TM) has been observed in DIII-D [15], and also fast-ion losses induced by neoclassical TM have been measured in ASDEX-U [16].

To study fast-ion losses, a new scintillator-based lost-fast ion probe has been developed in the HL-2A tokamak [19]. The design of the fast-ion loss probe is based on the concept of the α-particle detector used for the first time in TFTR and more recently in other major fusion devices. Compared with the fast-ion loss probe in the other devices, the new improvements are that the probe is capable of travelling across an equatorial plane port, and sweeping the aperture angle rotationally with respect to the axis of the probe shaft by two step motors, the radial position, and the collimator angle of the probe can be optimized. The high time resolution of the measurement has allowed the study of the fast-ion behaviour during MHD perturbations.

2. Experimental setups

The HL-2A device shown in figure 1 is a medium-size tokamak with closed divertor chambers [17]. The main parameters of HL-2A are major radius $R = 1.65$ m, minor radius $a = 0.4$ m, and plasma current (I_p) up to 0.5 MA. Sixteen toroidal field coils can create and maintain a toroidal magnetic field (B_t) up to 2.8 T. The magnetic field is directed to be clockwise (top view), whereas the plasma current is oriented to be counter-clockwise in the standard operation. The divertor of the device is characterized with two closed divertor chambers and at present it is operated with a lower single null configuration.

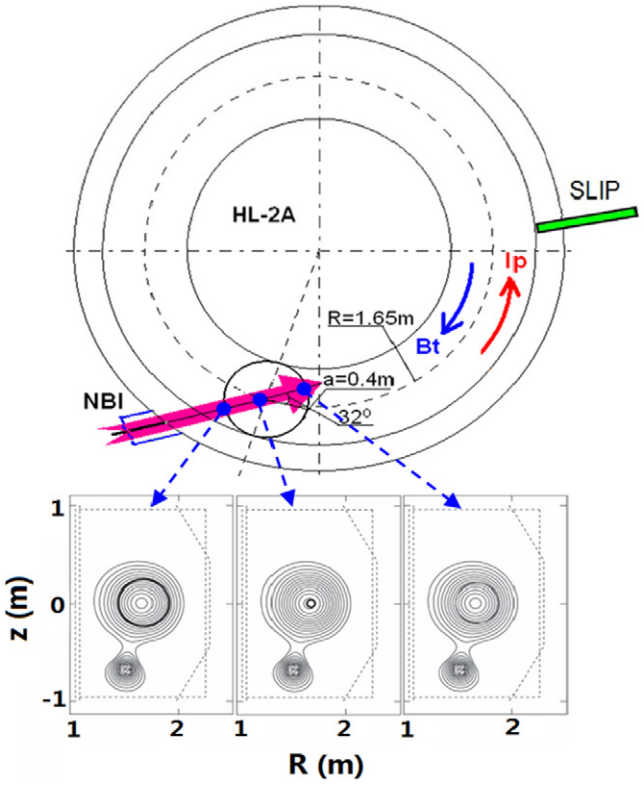

Figure 1. Arrangement of the NBI system and the fast-ion loss probe together with the calculation results of the NBI beam ions obtained by the Lorentz orbit code.

An NBI is installed on the HL-2A tokamak with four-positive-ion sources [18]. Each ion source consists of a multi-pole plasma generator and an accel–decel extraction system. The beam injection energy is typically 40 keV and a total beam power of up to 2.0 MW is delivered. The neutral beam is tangentially co-injected with a tangency radius 1.4 m. The deuterium neutrals are injected into the target plasma at an angle of 32° with respect to the plasma current at the magnetic axis. The initial beam ion velocities are therefore not perfectly parallel to the magnetic axis. The arrangement of the NBI system together with the fast-ion loss probe is schematically depicted in figure 1. In this experiment, a pulse neutral deuterium beam with the duration of ~500 ms was tangentially co-injected into target deuterium plasma. The main parameters of this experiment are shown in table 1. The Lorentz orbit code called LORBIT [19, 20] was modified for the HL-2A to check the class of initial beam-ion orbit right after ionization in the HL-2A tokamak. The LORBIT solves full gyromotion on EFIT equilibrium by using the Runge–Kutta method. Therefore, the code is full orbit code. Full gyromotion following orbits are tracked in the cylindrical system (R, Z, Φ). This code uses equilibrium data, i.e. the poloidal flux function $\Psi(R, Z)$ calculated by the EFTT code to produce the axisymmetric poloidal field components $B_R(= -(d\Psi/dZ)/R)$ and $B_Z(= (d\Psi/dR)/R)$. Currently, the TF ripple due to the finite number of toroidal coils is not considered. Figure 1 also shows three typical orbits of beam ions ionized at different locations on the NBI line. The calculation indicates that the initial orbits of beam ions are classified into passing orbits in the HL-2A plasma.

Table 1. Main parameters in the fast-ion loss experiment in HL-2A.

Plasma current, I_p	150–200 kA
Central line-averaged electron density, n_e	$(1.0–3.5) \times 10^{19}$ m^{-3}
Electron temperature, T_e	0.7–1.8 keV
Toroidal magnetic field, B_t	1.3 T
Plasma edge safety factor, q_{95}	4.0–6.0
Effective ionic charge, Z_{eff}	2.0–3.0
NBI power and pulse width	0.7–1.0 MW, 500 ms

A new scintillator-based lost fast-ion probe (SLIP) has recently been developed and operated in the HL-2A tokamak [19]. The fast-ion loss probe plays an important role in fast-ion experiments, detecting the fast-ion loss rate together with the Larmor radius ρ_i and pitch angle χ, from which the energy of the lost fast ions can be inferred: Namely $\rho_i = (2m_iE)^{1/2}/B_Lq$ and $\chi = \arccos(v_\parallel/v)$. Here, m_i, B_L, q, $v_\parallel$ and v represent the ion mass, the local magnetic field at the SLIP head position, the electric charge, the velocity component of the ions parallel to the magnetic field, and the velocity of the ions, respectively. Fast-ion loss probes have been developed in many devices [21–25]. The SLIP is installed at the equatorial on the outboard side of the tokamak. The distance between the detector head of the SLIP and the last closed magnetic flux surface is about 3 cm. The detector head is capable of moving into and withdrawing from the HL-2A vacuum chamber, and sweeping the aperture angle rotationally by the magnetic coupling drive system, in order to optimize the radial position and the collimator angle. The scintillator comprises ZnS : Ag (P11), which is deposited on a 25 mm × 25 mm aluminium substrate. The ranges of the E and χ that can be detected by the SLIP are 10–70 keV and 50°–85°, respectively. The light pattern on the scintillator plate is measured with a high-speed video camera. The frame rate of the camera using full pixel (1280 × 800) can be up to 7500 fps. This probe can provide information on the gyroradius centroid, i.e. the energy and the pitch angle of lost fast ions simultaneously if a two-dimensional image of scintillation light intensity due to the impact of the lost fast ions is measured.

In addition, the following HL-2A diagnostics are applied to the experimental analysis: MHD instability measurements with Mirnov coil arrays, electron temperature measurements with Thomson scattering diagnostics, line-averaged electron density measurements with a multi-channel HCN far-infrared laser interferometer, Mode identification with SXR tomography, and neutron emission measurements with a ^{235}U fission chamber neutron flux monitor (NFM).

3. Experimental results

In the 2013 HL-2A experimental campaign, the losses of neutral beam ions induced by MHD instabilities were measured and studied by means of the fast-ion loss probe. The used frame rate of the fast camera during this experiment was 1k fps. The MHD modes are faster (5–10 kHz) compared to the diagnostic resolution shown. Therefore, the measurement results are the integrated losses and some information on the fast-ion losses due to the MHD modes can be obtained. A photomultiplier (PMT) array is being developed for the fast-ion loss probe and the system can detect the total loss rate of fast ions as a function of time with frequency response up to 1 MHz. The PMT array will be available in the next campaign. The toroidal and poloidal mode number, frequency, and amplitude of MHD instabilities were indentified with arrays of Mirnov coils mounted inside the vacuum vessel.

The time evolution of the images of fast-ion losses due to TM was observed during a NBI discharge, as shown in figure 2. The plasma current is approximately 180 kA, and the central line-averaged electron density and the central electron temperature are about 3.0×10^{19} m^{-3} and 1.0 keV, respectively. A NBI pulse of 0.7 MW is injected into the ohmic plasma during the current flat-top phase, and the duration is 500 ms. During the MHD-quiescent phase, the fast-ion loss pictures look identical to image t_1. This image shows a single luminous spot consistent with losses at a single energy and pitch angle. This spot first appears when the NBI source is turned on and interpreted as the prompt losses of beam ions. Figure 3 is the prompt losses simulations of beam ions for shot 22493 obtained from LORBIT calculations. The energy and pitch-angle of the beam ions for the simulations are detected by the fast-ion loss probe. The ion grad-B drift direction is downward because B_t is directed to be clockwise (as seen from the top) in HL-2A. Banana beam ions will be lost at the outboard side of the lower plane in the HL-2A tokamak. The position and size of this spot is steady during the whole NBI heating. The energy and pitch angle of the lost beam ions due to prompt losses are approximately 40 keV and 63°, respectively. The acceleration voltage of the NBI system in HL-2A is about 40 kV. Accordingly, the measurement results are in good agreement with the full beam energy particles that have predominantly perpendicular velocities.

During NBI, the MHD instabilities are excited and then last for 60 ms. The singular value decomposition for the soft x-ray signals indicates the toroidal and poloidal mode numbers are $m/n = 2/1$. Figure 4 shows the soft x-ray tomography reconstruction during the instability for shot 22493. It can be seen that there are two islands during the instability which appear in the SXR emissivity. The time–frequency spectrum of this instability has been obtained by wavelet analysis, as shown in figure 2. It can be found that the frequency is about 5 kHz. According to the above analysis and soft x-ray tomography reconstruction, this instability was identified as TM. From figures 2(t_2) and (t_3), it can be seen that another luminous spot appears on the scintillator plate during TM. Along with the disappearance of the TM, the spot dims and then vanishes, as shown in image t_4. It is therefore reasonably concluded that the second light spot strongly correlates with TM, that is, the fast-ion loss event is induced by TM. Moreover, the spot becomes brighter as the TM amplitude becomes stronger, suggesting that the fast-ion losses increase with the increase in TM amplitude. The amplitude of the magnetic island can be estimated by the ratio of the amplitude of the perturbation to that of the equilibrium component. Alternatively, it can also be estimated by the singular values of the SVD analysis,

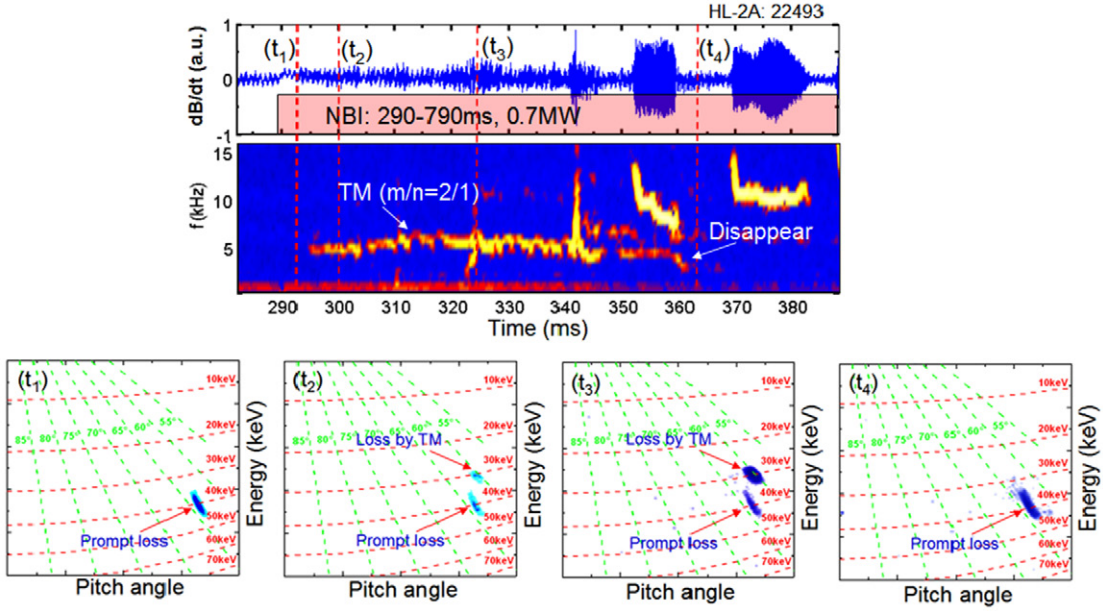

Figure 2. Typical fast-ion losses induced by TM in HL-2A. The upper panel shows the magnetic probe signal and its frequency spectrogram, with frame intervals of the fast-ion loss probe demarcated by vertical lines. The corresponding fast-ion loss distribution images at each time interval are shown in the lower panel. Details of the energy of the pitch angle of the lost ions have been mapped.

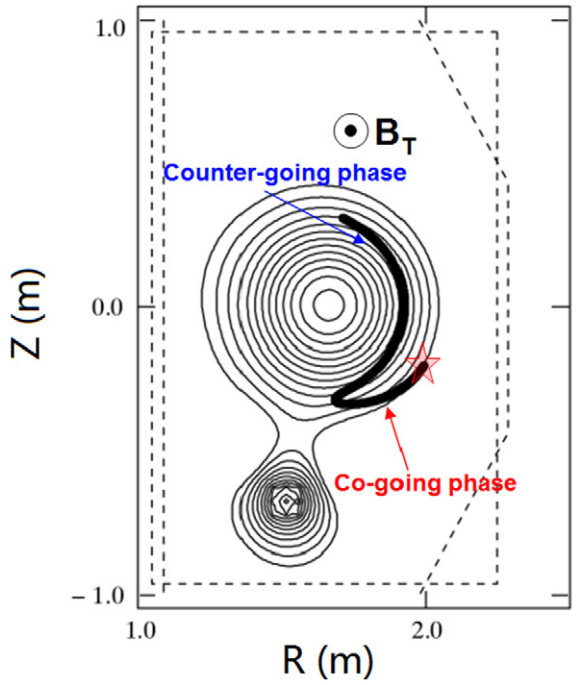

Figure 3. Prompt losses simulations of beam ions for shot 22493 obtained from LORBIT calculations.

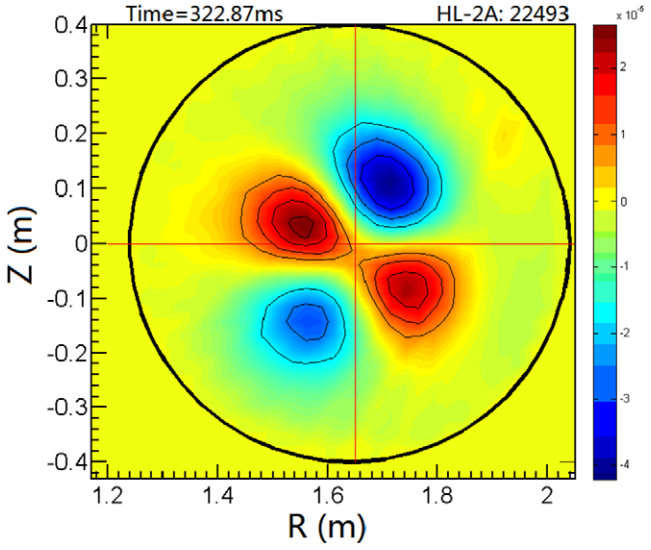

Figure 4. SXR tomography reconstruction during TM for shot 22493. Two islands appear in the SXR emissivity during the TM phase.

which provides the significance/energy of the equilibrium and perturbation components. Figure 5 shows the dependence of the integrated losses normalized by the maximum fast-ion loss populations induced by TM on the mode amplitude. As shown in figure 5, it can be seen that the fast-ion loss rate increases as the MHD magnetic fluctuation amplitude increases as observed. The position of the second spot in the scintillator plate is located in the region with lower energy and a lower pitch angle, in contrast to the first spot due to prompt losses. The energy and pitch angle of the lost fast ions induced by TM are 30 keV and 60°, respectively.

Actually, the spot in figure 2 is somewhat broad around the value of 30 keV and 60°, which is due to the limited energy and pitch-angle resolutions of the fast-ion loss probe. The energy resolution of the fast-ion loss probe is determined by the height of the apertures. The pitch-angle resolution of the probe is decided by the width of the front aperture. The resolution with the current collimator geometry has been calculated, and the results are shown in figure 6. Figure 6(*a*) shows the calculated gyroradius distributions for 10, 15, and 20 mm at a pitch angle of 60°. The full widths at half maximum (FWHM) for this set of gyroradii are 2.0, 3.2, and 4.4 mm, respectively.

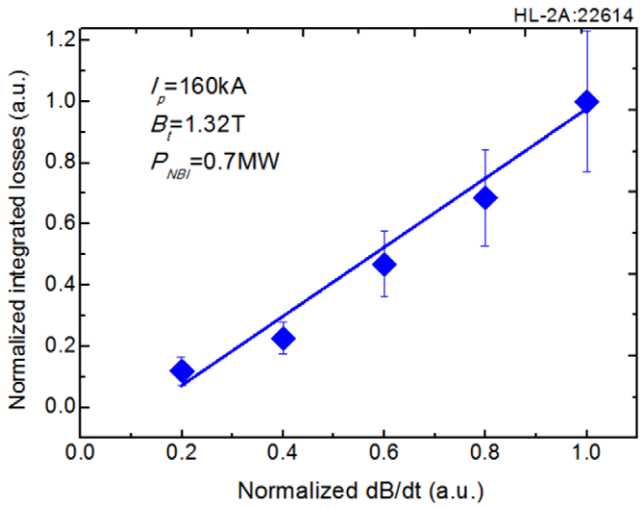

Figure 5. Integrated fast-ion loss rate as a function of normalized TM mode amplitude. The statistic trend of the fast-ion loss rate versus mode amplitude is well consistent with the expected scenarios.

It can be seen that the energy resolution becomes worse with increasing energy, which implies that the collimating effect of the 3D collimator becomes weaker for the ions with higher energy. Figure 6(*b*) shows the calculated pitch angle distributions for 80, 70, and 60 at a gyroradius of 20 mm. The results indicate that the pitch angle resolution is better than the energy resolution and the probe has the same FWHM ≈5° for all pitch angles. Therefore, the measured spot is somewhat broad around the actual value.

The time evolution of the images of fast-ion losses due to long-lived mode (LLM) and sawtooth crashes was also measured during the same discharge, as shown in figure 7. Long-lived saturated internal modes, observed on many devices [26–28], are thought to originate from the pressure gradient in plasmas with a safety factor profile having either a weakly reversed shear or a broad low-shear region. These modes often cause rotation flattening in the plasma core, and degrade fast-ion confinement and plasma stored energy. The oscillations show dependence on both the safety factor profile and the plasma pressure gradient, and energetic particles (EPs) also play an important role. Figure 8 shows the soft x-ray tomography reconstruction during LLM for shot 22614. It can be seen that there is an island during LLM ,which appears in the SXR emissivity. By comparing figures 4 and 8, it can be seen that the amplitude of the magnetic island of LLM is higher than that of TM. The measurement results from the fast-ion loss probe show that the brightness of the luminous spot due to LLM is brighter than that due to TM, which suggests that the fast-ion loss rate induced by LLM is higher than that induced by TM. That is, the deleterious effect of LLM on the confinement of fast ions is stronger that the effect of TM. The SXR tomography reconstruction results are well consistent with the measurement results. The energy and pitch angle of the lost fast ions induced by LLM are 32 keV and 67°, respectively. Sawtooth oscillations are periodic, MHD initiated mixing events that occur in a tokamak plasma in the near axis region where the safety factor q is less than or equal to unity. Compared with the luminous spots due to TM and LLM, the spot induced by sawtooth has a broad range of energies and pitch angles. The energy of the sawtooth crash-induced lost fast-ions ranges from 27 keV to 38 keV, and the pitch angle ranges from 63° to 72°. The brightness of the luminous spot due to LLM is significantly weaker than the brightness of the spot due to sawtooth, which implies that the deleterious effect of sawtooth on the confinement of fast ions is obviously stronger than the effect of LLM. In addition, fast-ion loss rate increases as the MHD magnetic fluctuation amplitude increase as expected. Sawtooth oscillations are the result of internal reconnection events that locally break the magnetic topology and cause a sudden loss of confinement. There may be some interactions between sawtooth oscillations and fast ions, which causes the fast-ion losses with the wide range of pitch angle. An additional concern in a fusion-burning plasma is that if the sawtooth period is shorter than the slowing down time of the fusion alpha particles then the fusion alphas may be scattered, and perhaps lost, before they have time to transfer their energy to the thermal plasma. Therefore, the best sawtooth regime for ITER would be one where the sawtooth period is intermediate between the alpha particle slowing down time and the plasma heating (or energy confinement) time.

Disruptions are a major concern for tokamaks, not just for present-day machines, but even more so for ITER and future tokamak reactors [25]. During disruptions, both plasma-stored-energy and the energetic ions are released drastically to the plasma facing components. The phenomenon poses a serious threat to the safe operation of a fusion reactor. Therefore, plasma disruptions in tokamaks have been extensively investigated [29–31]. However, previous studies have mainly focused on the disruption-produced runaway electrons.

Major disruption has two types: Fast disruption and slow disruption. For the first case, the magnetic confinement is completely lost. The plasma discharge is quickly terminated (~3 ms for HL-2A). Therefore, during this type of disruption, the confinement is completely lost for ions. For the second case, the magnetic confinement is not completely lost. During the initial stage of the disruption, the confinement is severely lost. Then, the confinement is recovered and the magnetic configuration is in a special stable state. A runaway electron beam can be well constrained in this configuration. This experimental phenomenon has been observed in the HL-2A tokamak [28].

In this experiment, the fast ion losses during the second type of disruption have been studied. The images of the fast-ion losses during disruptions with NBI have been measured by the SLIP. A typical disruption discharge with NBI is shown in figure 9, where the temporal evolution of the main parameters is plotted for shot 22614. A NBI pulse with 1 MW is injected into plasma from 610 to 843 ms. A major disruption occurs at 832 ms and ends up at 848 ms. Figure 9(*b*) shows the evolution of the neutron emission rate before and during this disruption. With the start of the disruption, the neutron emission rate decreases sharply. Moreover, with the shutdown of the NBI, the neutron emission rate quickly drops to a very low level (almost zero). This evidence indicates that fusion neutrons are produced during disruption with NBI. From figure 9(*b*), it can

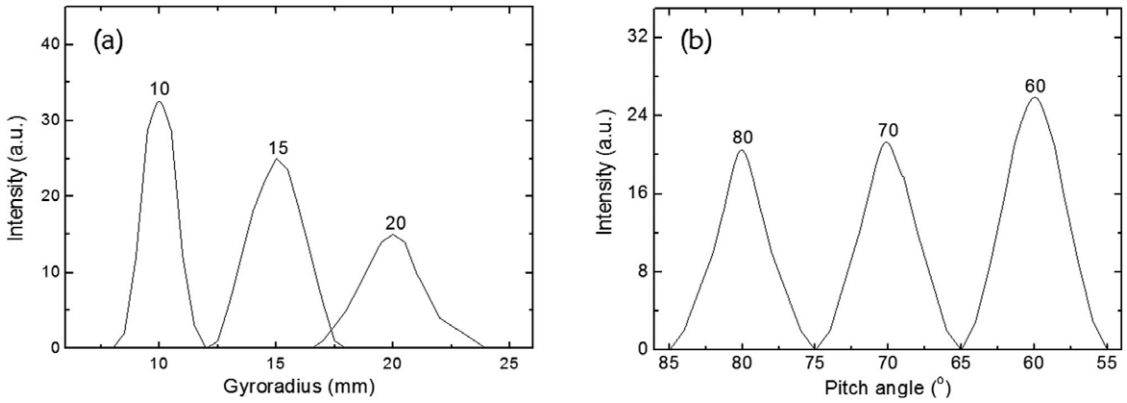

Figure 6. (*a*) The calculated gyroradius centroid distributions for 10, 15, and 20 mm at a pitch angle of 60° and (*b*) the calculated pitch angle distributions for 80°, 70°, and 60° at a gyroradius of 20 mm.

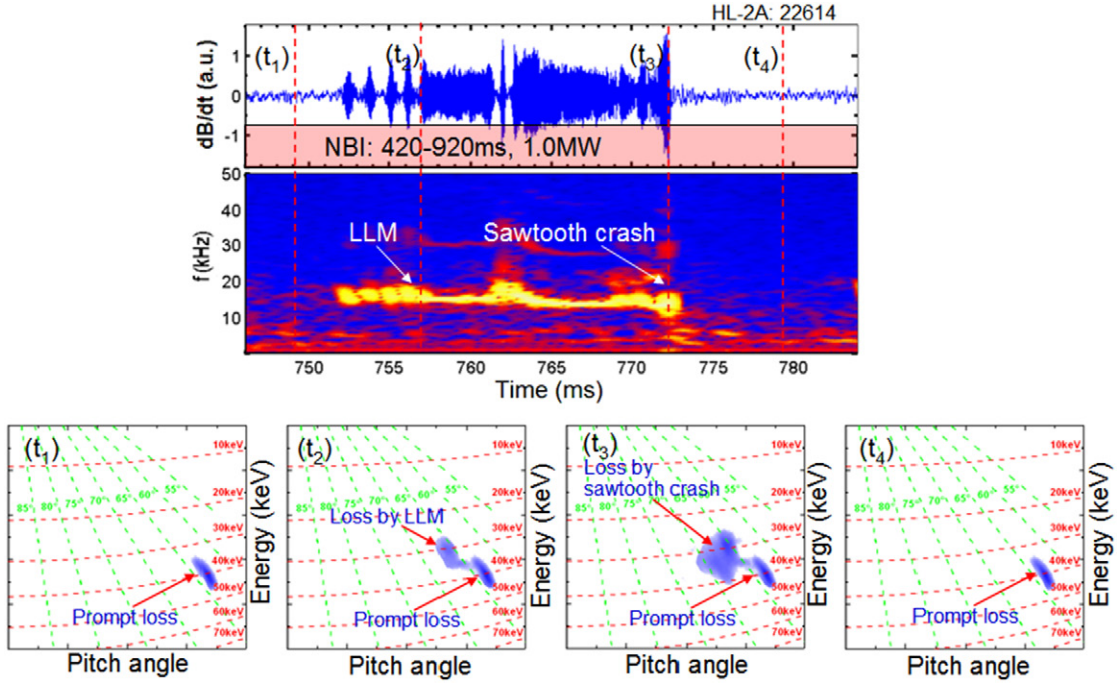

Figure 7. Typical fast-ion losses induced by LLM and sawtooth crash in HL-2A. The upper panel shows the magnetic probe signal and its frequency spectrogram, with frame intervals of the fast-ion loss probe demarcated by vertical lines. The corresponding fast-ion loss distribution images at each time interval are shown in the lower panel. Details of the energy of the pitch angle of the lost ions have been mapped.

be seen that the total neutron rate drops by ~90% as a result of the disruption, which implies that a significant fraction of the fast ions is lost from the plasma. The NBI source is maintained for about 10 ms during the disruption, which provides an opportunity to study the fast-ion behaviour during the disruptions. The frame rate of the fast camera we used for this shot is 1 kfps. Therefore, some images of the beam-ion losses during the disruption can be obtained.

Figure 10 shows two beam-ion-loss images on the scintillator screen before and during the disruption, respectively. Before the disruption, there is only a luminous spot due to the prompt losses on the screen. During the disruption, the scintillation light spot on the screen is significantly changed. Firstly, the brightness of the light spot is largely enhanced, indicating that the losses of the NBI beam ions dramatically increase during the disruption. Note that the present results provide clear experimental evidence for the enhancement of fast-ion losses during a disruption stage. Secondly, the shape of the light spot is changed tremendously and the area of the spot increases obviously during the disruption. A possible reason is that the transport of beam ions from the plasma core to the edge varies dramatically during the disruption because of strong magnetic perturbations and the change in the plasma current profile.

Magnetic measurements and EFIT calculation can provide some important information about the magnetic perturbation and the evolution of the magnetic configuration. Figure 11 shows the magnetic configuration reconstructions during different phases. It can be seen that the magnetic field structures during TM, Sawtooth crash, and LLM are almost not changed, but during disruption it is changed greatly. Therefore, the fast-ion transport from the plasma core to the edge is changed dramatically during disruptions. In addition, Magnetic

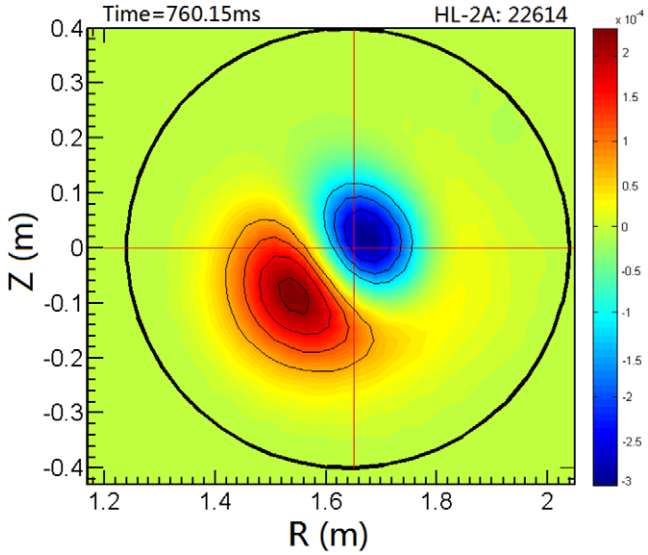

Figure 8. SXR tomography reconstruction during LLM for shot 22614. An island appears in the SXR emissivity during the LLM phase.

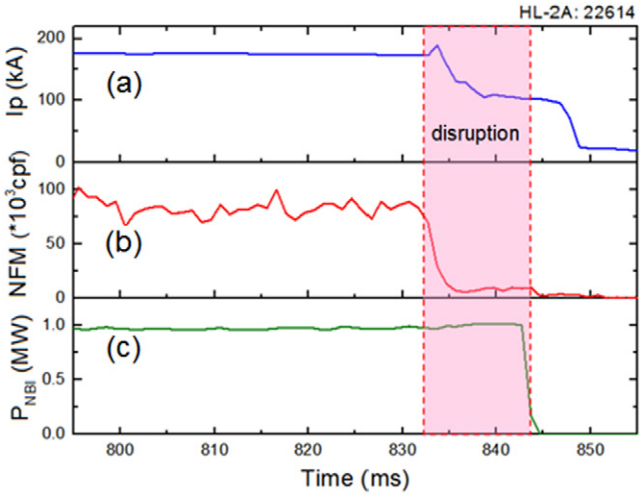

Figure 9. Time traces of the plasma current I_p (*a*), neutron emission rate NFM (*b*) and NBI power P_{NBI} (*c*) in a major disruption with NBI. The shaded area indicates the time interval in which the disruption with NBI occurs. The total neutron rate drops by ~90% as a result of the disruption occurrence.

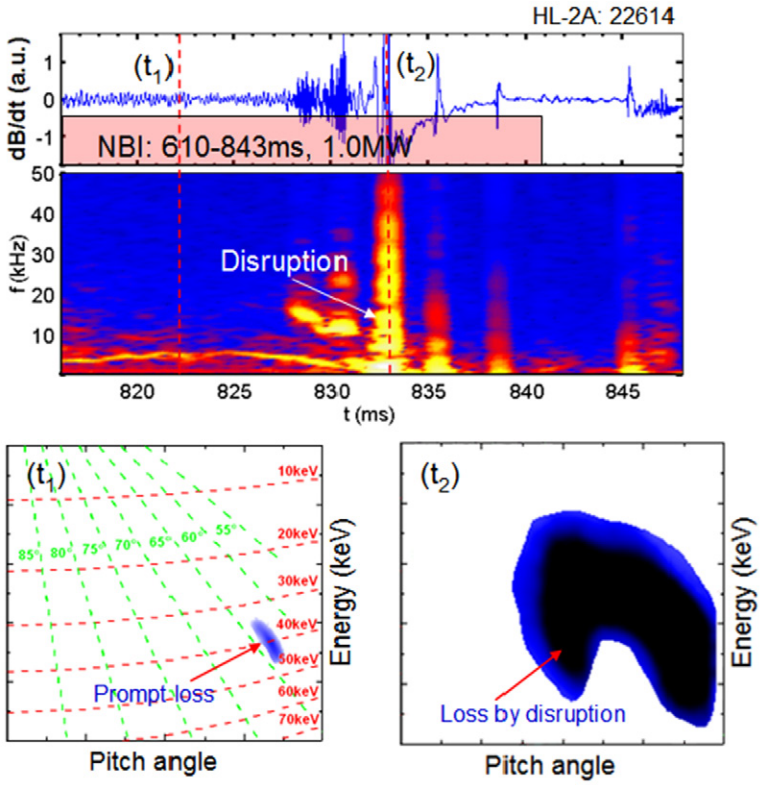

Figure 10. Typical fast-ion losses induced by disruption in HL-2A. The upper panel shows the magnetic probe signal and its frequency spectrogram, with frame intervals of the fast-ion loss probe demarcated by vertical lines. The corresponding fast-ion loss distribution images at each time interval are shown in the lower panel. Details of the energy of pitch angle of the lost ions have been mapped for the t_1 image. The map is not available during the disruptions.

measurements show that the magnetic perturbation amplitude near the fast-ion loss probe head during TM, sawtooth crash, and LLM is very small ($<10^{-3}$ T), but during disruption it is very big ($>10^{-1}$ T). The map of energy versus pitch angle for the fast-ion loss probe is calculated and obtained. An important parameter for the calculation is the magnetic configuration near the probe head. Moreover, a very important assumption for the map calculation is that the magnetic configuration is in a steady state. Since the map of energy versus pitch angle is only available under quasi-steady state conditions, the map is not available if the magnetic perturbation amplitude is sufficiently high. Accordingly, the map of energy versus pitch

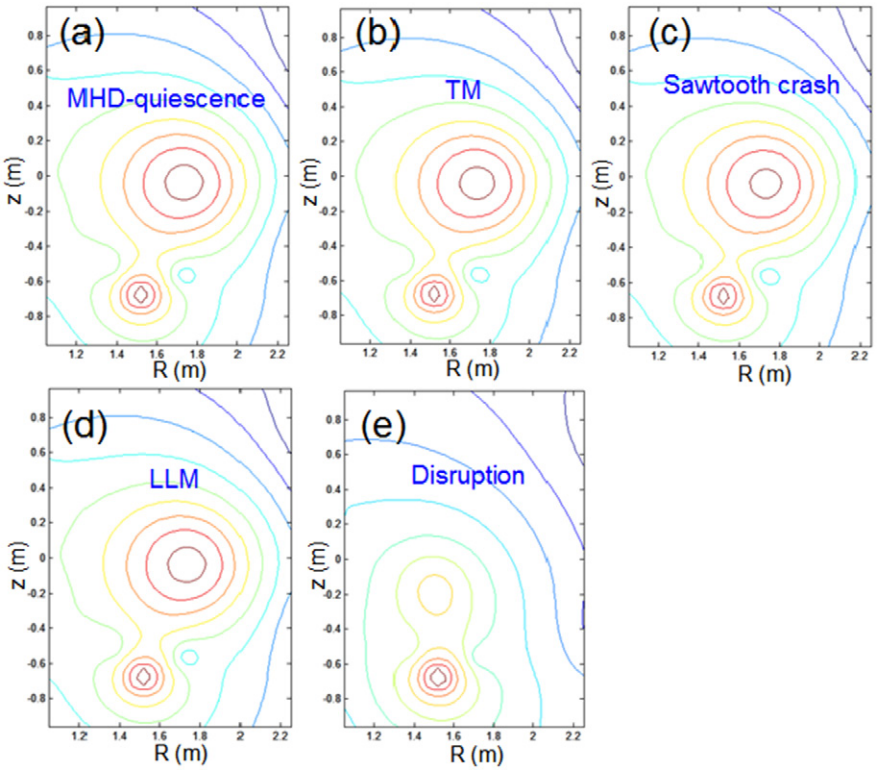

Figure 11. Magnetic configuration reconstructions using the EFIT code during (*a*) MHD-quiescence, (*b*) TM, (*c*) sawtooth crash, (*d*) LLM, and (*e*) disruption.

angle is available during TM, Sawtooth crash, and LLM, but is not available during disruptions.

4. Conclusions

Fast-ion losses induced by MHD instabilities have been measured and studied in the HL-2A tokamak by means of a new SLIP. Experiments have shown that the fast-ion loss rate increases as the MHD magnetic fluctuation amplitude increases as expected. Measurements show that the energy and pitch angle of the lost ions due to TM are 30 keV and 60°, respectively, and that due to LLM they are 32 keV and 67°, respectively. Compared with TM and LLM, the spot induced by sawtooth has a broad range in energy and pitch angle. The energy of the sawtooth-induced lost fast-ions ranges from 27 keV to 38 keV, and the pitch angle ranges from 63° to 72°. There may be some interactions between MHD instabilities and energetic ions, which causes the fast-ion losses with the wide range of energy and pitch angle. The total neutron rate drops by ~90% as a result of the disruption, which implies that a significant fraction of the fast ions is lost from the plasma during disruptions. Clear experimental evidence of the drastic loss of beam ions during disruptions was obtained by the probe. Possible reasons for this phenomenon are the strong magnetic perturbations and the drastic change in the fast-ion transport.

In the next generation of tokamak, the threat of fast-ion losses due to MHD instabilities is becoming more dangerous with the increase in population and energy. Moreover, if the MHD instability period is shorter than the slowing down time of the fusion alpha particles then the fusion alphas may be scattered and lost before they have time to transfer their energy to the thermal plasma. Therefore, the development of effective methods for the control or mitigation of the fast-ion loss induced by MHD instabilities is a critical task.

Acknowledgments

The authors deeply appreciate the cooperation and assistance of the discharge operation group and the NBI group of the HL-2A tokamak. One of the authors, Y.P. Zhang, expresses sincere gratitude to Professor W.W. Heidbrink, Professor L. Zheng and Dr Dong Li for their valuable support and helpful discussions.

This work was partially supported by the National Science and Technology Major Project of the Ministry of Science and Technology of China (Grant Nos 2013GB106004, 2014GB109000 and 2014GB109003), the National Natural Science Foundation of China (Grant Nos 11005036 and 11375004), and it was also partially supported within the framework of the cooperation between the Japan Society for the Promotion of Science (JSPS) and Chinese Academy of Science (CAS) Core-University Programme in the field of 'Plasma and Nuclear Fusion'.

References

[1] Heidbrink W.W. *et al* 1988 *Nucl. Fusion* **28** 1897
[2] Heidbrink W.W. 1990 *Phys. Fluids* B **2** 4
[3] Isobe M. *et al* 1997 *Nucl. Fusion* **37** 437
[4] Pinches S.D. *et al* 2004 *Plasma Phys. Control. Fusion* **46** B187
[5] García-Muñoz M. *et al* 2008 *Phys. Rev. Lett.* **100** 055005

[6] Forest C.B. *et al* 1997 *Phys. Rev. Lett.* **79** 427
[7] Darrow D.S. *et al* 1996 *Nucl. Fusion* **36** 509
[8] Fu G.Y. *et al* 1989 *Phys. Fluids* B **1** 1949
[9] Wong K L. 1999 *Plasma Phys. Control. Fusion* **41** R1
[10] Fasoli A. *et al* 2007 Progress in the ITER Physics Basis: chapter 5. Physics of energetic ions *Nucl. Fusion* **47** S264
[11] Heidbrink W.W. *et al* 2009 *Phys. Rev. Lett.* **103** 175001
[12] Zhang Y. P. *et al* 2012 *Phys. Plasmas* **19** 112504
[13] Chen X. *et al* 2013 *Phys. Rev. Lett.* **110** 065004
[14] Nave M.F.F. *et al* 2002 *Nucl. Fusion* **42** 281
[15] Carolipio E.M. *et al* 2002 *Nucl. Fusion* **42** 687
[16] Garcia-Munoz M. *et al* 2007 *Nucl. Fusion* **47** L10
[17] Yan L.W. *et al* 2011 *Nucl. Fusion* **51** 094016
[18] Liu H. *et al* 2009 *Plasma Sci. Technol.* **11** 613
[19] Zhang Y.P. *et al* 2014 *Rev. Sci. Instrum.* **85** 053502
[20] Isobe M. *et al* 2009 *J. Plasma Fusion Res. Ser.* **8** 330
[21] Zweben S.J. 1989 *Nucl. Fusion* **29** 825
[22] Isobe M. *et al* 1999 *Rev. Sci. Instrum.* **70** 827
[23] Garcia-Munoz M. *et al* 2009 *Rev. Sci. Instrum.* **80** 053503
[24] Darrow D.S. 2008 *Rev. Sci. Instrum.* **79** 023502
[25] Erisson L.-D. *et al* 2004 *Phys. Rev. Lett.* **92** 205004
[26] Gryaznevich M.P. *et al* 2008 *Nucl. Fusion* **48** 084003
[27] Chapman I.T. *et al* 2010 *Nucl. Fusion* **50** 045007
[28] Deng W. *et al* 2014 *Nucl. Fusion* **54** 013010
[29] Hender T.C. *et al* Progress in the ITER Physics Basis: chapter 3. MHD stability, perational limits and disruptions 2007 *Nucl. Fusion* **47** S128 (beginning of chapter)
[30] Esposito B. *et al* 2008 *Phys. Rev. Lett.* **100** 045006
[31] Zhang Y.P. *et al* 2012 *Phys. Plasmas* **19** 032510